2017

Nanjing University of Aeronautics and Astronautics

Universitat Politècnica de Catalunya (EEBE)

Guillem Roca

AIRCRAFT TURNING GROUND MANEUVERS

Abstract

In this project a fully parameterized mathematical model of an aircraft turning on the ground in order to get the maximum aircraft speed and minimum infrastructure taxiway radius for three different types of aircrafts (A320, A380 and B737) is developed.

The mathematical model takes the form of a system of coupled ordinary differential equations (ODEs). The airframe is considered as a rigid body with six DOF and the equations of motion are derived by balancing the respective forces and moments. Other formulas as Newton's second law, centripetal equations, friction formulas and other equations will be used to calculate the safest velocity depending on the radius of the taxiway curvature.

The software Matlab will be used so as to make all the calculations and will enable us to change the parameters such as mass, friction or radius to find new velocities according to the aircraft. Moreover, the use of Microsoft Excel software to insert those results already found in Matlab and create new tables depending on the radius and ground weather conditions (dry or wet). The results show that each aircraft has a different safety velocity although they turn with the same taxiway radius.

There is also a bibliographic and modelling work explaining how to get all the equations and the different types of taxiway entries.

Acknowledgements

I would like to thank my supervisors Dr. Ye Bojia and Dr. Tian Yong for their continued support and encouragement. Without their guidance and expertise this Final Year Project would not have been possible.

I am especially grateful with Marc Saez, who took care of me after a surgery operation in China.

Thanks also to my friend Marc Rosique and everyone that made my time unique in Nanjing, China.

Contents

List of figures

List of tables

List of equations

Nomenclature

l_{xN}: x-distance to the nose gear

l_{zN}: z-distance to the nose gear

$l_{xR,L}$: x-distance to the main gears

$l_{yR,L}$: y-distance to the main gears

$l_{zR,L}$: z-distance to the main gears

l_{xA}: x-distance to the aerodynamic center

l_{zA}: z-distance to the aerodynamic center

l_{xT}: x-distance to the thrust center

$l_{yTR,TL}$: y-distance to the thrust center

l_{zT}: z-distance to the thrust center

m: Mass of the aircraft

k_{zN}: Stiffness coefficient of the nose gear

k_{zM}: Stiffness coefficient of the main tyre

c_{zN}: Damping coefficient of the nose tyre

c_{zM}: Damping coefficient of the main tyre

μ_R: Rolling resistance coefficient

l_{mac}: Mean aerodynamic chord

S_w: Wing surface area

ζ: Damping ratio

V_x, V_y, V_z: Velocities about the axes x, y and z

W_x, W_y, W_z: Rotational velocities about the axes x,y,z

V_{zN}: Vertical velocity of the nose gear

α: Slip angle

R: Radius

N: Normal force

g: Gravity

F_f: Fiction force (changes if the ground is dry or wet)

a: Acceleration

δ: Deflection of the tyre

I_x, I_y, I_z: Moment of inertias about the axes x, y and z

1. Introduction

Driving at excessive speed during ground maneuvers may force the aircraft to enter in a spin and endanger the life of many passengers. That is the reason why pilots and air traffic controllers take speeding controls measures when turning.

The aim of this research is to avoid any kind of accident in airports by calculating the maximum speed that an aircraft can reach with a given curved taxiway radius. Those calculations are made with the Aircraft 320, Aircraft 380 and Aircraft B737, which the 90% of the flights in many airports operate with these models of aircrafts.

The dynamics of an aircraft's ground handling are governed by many different aspects of its design, loading and operational practice. Factors such as the taxiway surface, weather conditions and tire wear also play an important role. This research also considers all the calculations when aircrafts are turning on a wet ground due to the rain effect. The idea is to use these velocity calculations for any airport depending on the radius, weather conditions and kind of aircraft (A380, A320 or B737).

From a commercial point of view, the speed at which taxing maneuvers are performed is important; since a reduction of time spent taxing improves efficiency of operations at airports. Control of aircraft on the ground is one of the few areas in which automation has not been employed. In the past, computer modeling has been an invaluable tool in studying the ground dynamics of aircraft due to the high cost of real ground tests. This project focuses on an investigation into the stability of ground maneuvers in aircrafts A380, A320 and B737 (90% of the airports operate with those three kinds of aircrafts).

A bibliographic investigation into high-speed taxiway exits is given, which have been in use at a number of airports and their purpose is to reduce the taxiway occupancy time.

Once the simulation design is presented, the results obtained are shown in some tables and explained.

Finally, the conclusions of the entire project are offered.

2. Bibliographic documentation

2.1. Types of entries

2.1.1.Conventional 90-degree Taxiway Entry

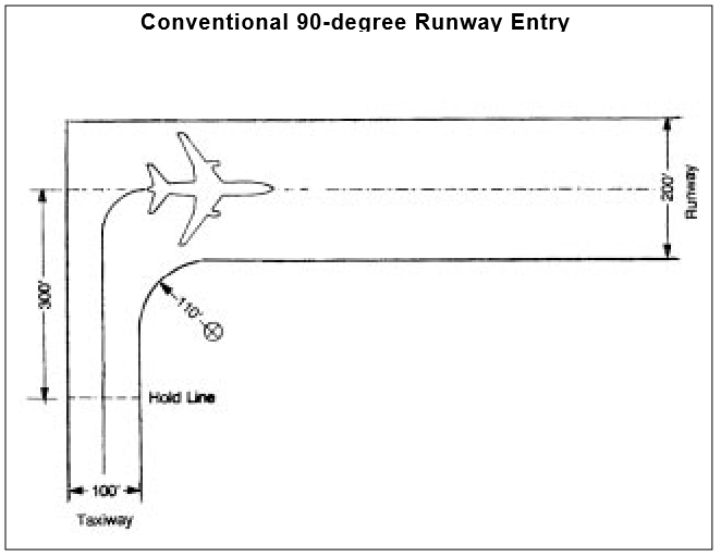

Figure 2-aConventional 90-degree Taxiway Entry[1]

With this type of entry, the aircraft enters the taxiway at a slow speed, because it must make a 90-degree turn through a curve with a short radius to line up on the taxiway central line. The aircraft will stop on the taxiway if takeoff clearance has not been received. In this case, the uncertainty about just when the aircraft will be started presents a problem for the air traffic controller and the controller usually will have allowed more than adequate separation before clearing the departure on to the taxiway in the first place. The use of this extra separation is prudent from the standpoint of safety, but it tends to increase the average taxiway interval, and thus reduces the airport capacity.[1]

2.1.2.Typical Rapid Taxiway Entry

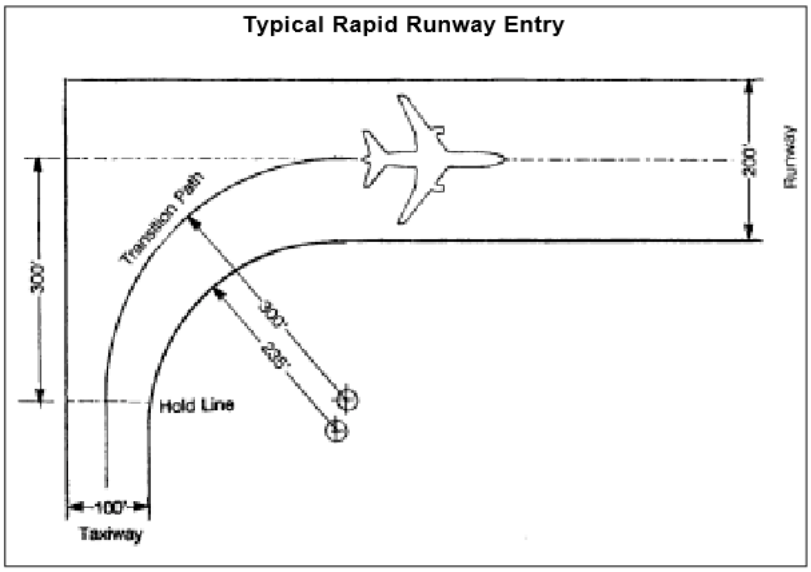

Figure 2-b Typical Rapid Taxiway Entry[1]

The operating procedure is based on the use of rolling take-offs to minimize the taxiway occupancy time. The hold line marked on the taxiway is offset the same distance from the taxiway central line as the hold line for a conventional 90-degree entry. As in the case of high-speed exit, the safe speed on the curved transition path depends upon the turn radius and the surface conditions. This procedure makes the actual take-off time much more predictable and allows the controller to minimize the actual separation between a departure and a following arrival. The only disadvantage about this type of entry is that an extra pavement is required. In this project all the calculations are done with this kind of entry, the typical rapid taxiway entry.[1]

2.2. Calculation of Minimum Line-Up Distance Correction

2.2.1.90° turn on taxiway entry

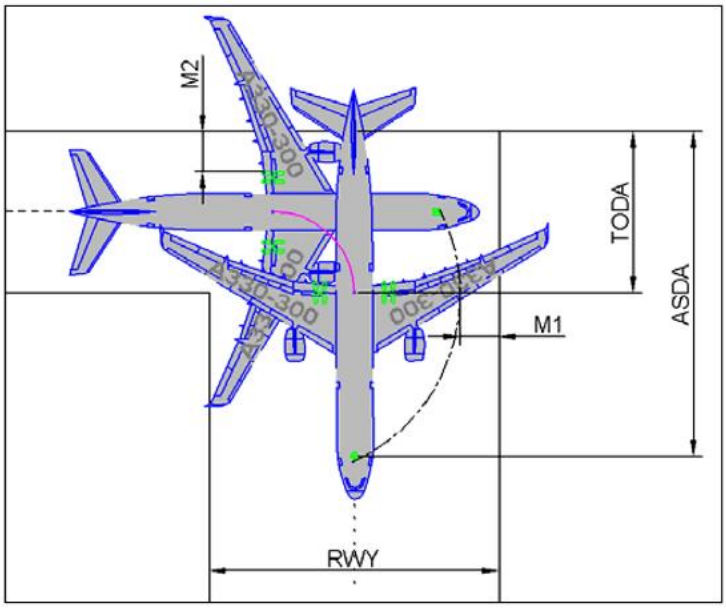

Figure 2-c Minimum Surface 90 Degree Turn[2]

This maneuver consists in a 90° turn at minimum turn radius starting with the Main Landing Gear (MLG) edge at a distance M2 from taxiway edge, and finishing with the aircraft aligned on the centerline of the taxiway.[2]

90° turn on runway entry															
Aircraft model	Max steering angle (degree)	30m wide runway				45m wide runway (STANDARD WIDTH)				60m wide runway					
		Minimum line-up distance correction				Minimum line-up distance correction				Minimum line-up distance correction					
		On TODA		On ASDA		On TODA		On ASDA		On TODA		On ASDA			
		feet	meters	feet	meters	feet	meters	feet	meters	feet	meters	feet	meters		
A318	75,0	36	10,8	69	21,1	Same as 30m				Same as 30m					
A319	75,0	36	11,1	73	22,1	Same as 30m				Same as 30m					
A320	75,0	38	11,7	80	24,3	Same as 30m				Same as 30m					
A321	75,0	46	13,9	101	30,8	41	12,6	97	29,5	Same as 45m					
A300	65,0	N/A				63	19,3	125	38,0	Same as 45m					
A310	65,0	N/A				57	17,3	107	32,5	Same as 45m					
A330-200 (1)	65,0	N/A				74	22,5	147	44,7	Same as 45m					
A330-200 (2)	72,0	N/A				65	19,7	137	41,9	Same as 45m					
A330-300 (1)	65,0	N/A				80	24,2	163	49,6	Same as 45m					
A330-300 (2)	72,0	N/A				69	21,2	153	46,5	Same as 45m					
A340-200 (1)	65,0	N/A				70	21,5	147	44,7	Same as 45m					
A340-200 (2)	72,0	N/A				61	18,6	137	41,8	Same as 45m					
A340-300 (1)	65,0	N/A				73	22,2	156	47,6	Same as 45m					
A340-300 (2)	72,0	N/A				67	20,5	151	45,9	62	19,0	146	44,4		
A340-500	70,0	N/A				80	24,5	172	52,5	73	22,1	164	50,1		
A340-600	76,0	N/A				110	33,6	219	66,8	67	20,5	176	53,7		
A350-800	72,0	N/A				69	20,9	150	45,8	Same as 45m					
A350-900	72,0	N/A				84	25,7	178	54,3	72	21,8	166	50,5		
A350-1000	75,0	N/A				106	32,2	212	64,7	72	21,9	179	54,4		
A380-800	70,0	N/A				94	28,6	192	58,5	75	22,8	173	52,7		

Table 2-a 90 Degree Turn Taxiway[2]

2.3. 180° turn on taxiway turn pad

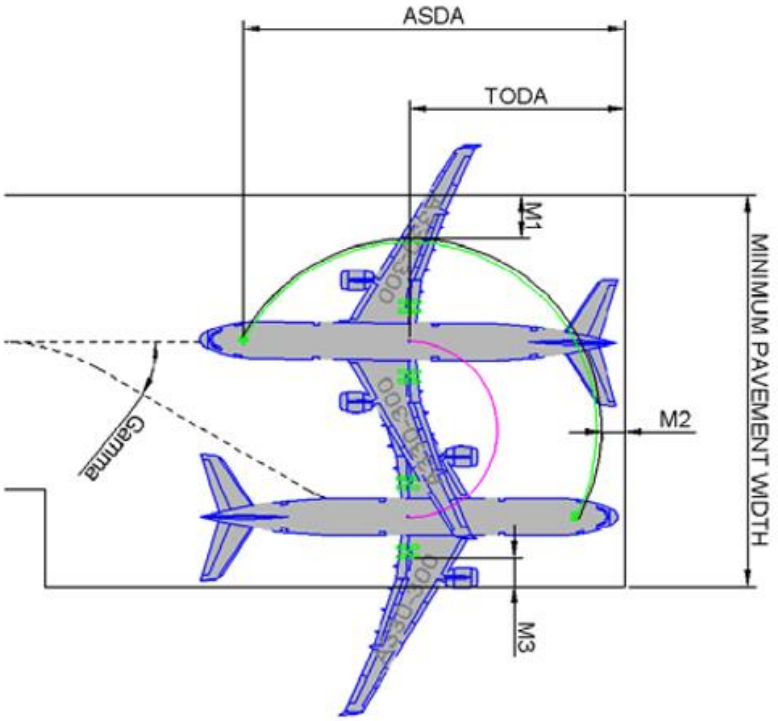

Figure 2-d Minimum Surface 180 Degree Turn[2]

This maneuver consists in a 180° turn on a standard ICAO taxiway turn pad geometry. It starts with MLG edge at a distance M3 from taxiway edge, and it finishes with the aircraft aligned on the centerline of the taxiway.[2]

180° turn on runway turn pad															
Aircraft model	Max steering angle (degree)	30m wide runway				45m wide runway (STANDARD WIDTH)				60m wide runway					
		Minimum line-up distance correction				Minimum line-up distance correction				Minimum line-up distance correction					
		On TODA		On ASDA		On TODA		On ASDA		On TODA		On ASDA			
		feet	meters	feet	meters	feet	meters	feet	meters	feet	meters	feet	meters		
A318	75,0	46	14,1	80	24,4	Same as 30m				Same as 30m					
A319	75,0	49	15,0	85	26,0	Same as 30m				Same as 30m					
A320	75,0	55	16,7	96	29,3	Same as 30m				Same as 30m					
A321	75,0	70	21,4	126	38,3	69	21,0	124	37,9	Same as 45m					
A300	65,0	N/A				85	25,8	146	44,5	Same as 45m					
A310	65,0	N/A				72	21,8	122	37,1	Same as 45m					
A330-200 (1)	65,0	N/A				99	30,1	171	52,2	Same as 45m					
A330-200 (2)	72,0	N/A				95	28,9	168	51,1	Same as 45m					
A330-300 (1)	65,0	N/A				111	33,7	194	59,1	Same as 45m					
A330-300 (2)	72,0	N/A				106	32,4	190	57,8	Same as 45m					
A340-200 (1)	65,0	N/A				100	30,5	176	53,7	Same as 45m					
A340-200 (2)	72,0	N/A				97	29,5	173	52,7	Same as 45m					
A340-300 (1)	65,0	N/A				108	32,8	191	58,2	Same as 45m					
A340-300 (2)	72,0	N/A				106	32,2	189	57,6	104	31,7	187	57,1		
A340-500	70,0	N/A				119	36,2	210	64,2	116	35,2	207	63,2		
A340-600	76,0	N/A				149	45,3	258	78,5	130	39,7	239	72,9		
A350-800	72,0	N/A				104	31,8	186	56,7	Same as 45m					
A350-900	72,0	N/A				122	37,2	216	65,9	117	35,7	211	64,4		
A350-1000	75,0	N/A				144	43,9	250	76,3	129	39,4	236	71,9		
A380-800	70,0	N/A				130	39,5	227	69,3	122	37,1	219	66,9		

Table 2-b 180 Degree Taxiway Turn[2]

2.4. Taxiway infrastructure requirement

In this section, there is brief explanation of the minimum width of a taxiway. This bibliographic information is only given for Airbus 380 because it is the biggest aircraft, and means that the other two types of aircrafts fit on the taxiway.

2.4.1.Minimum taxiway width

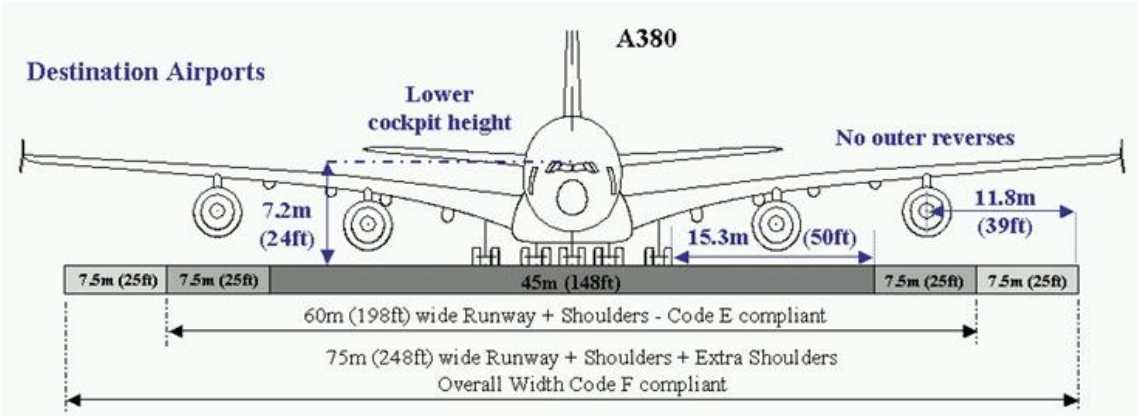

Figure 2-e Infrastructure requirements A380

It can be concluded that on a 23 meter code E (Annex 14)[3] taxiway the A380 can taxi safely under the condition that this taxiway is provided with proper guidance. Under these conditions no specific operational procedures is required. The other two types of aircrafts (A320 and B737) would suit perfectly according to this 23 m width due the fact that are smaller aircrafts.[4]

2.4.2.Width of curved taxiway A380

To facilitate the movement of an A380 on curved taxiways, fillets should be provided. The design of the fillet should ensure that a minimum wheel to edge clearance is maintained. ICAO[3] requires a minimum wheel to edge clearance of 4.5 meters for curved taxiway segments.[4]

2.5. Literature review

Few researches about ground maneuvers in aircrafts have been submitted due the fact that the accident risk of an aircraft is higher while flying than when turning on the ground.

Firstly, an old case study performed by Tirey k. Vickers (1991)[1], which studies aircraft effects on high-speed taxiways in order to reduce time. This case only shows few results for dry pavement and affirms that the safe taxiway exit speed depends on the radius of the turn that is used to enter the exit taxiway. In addition, another project carried out by J. Rankin (2010)[5] that has been useful for the modelling chapter. The objective of this work was to use a mathematical and computer modelling to study the dynamics of an aircraft moving on the ground. An efficient method was developed to identify safe operating conditions in order to inform operational practice and the design of automated control systems. Moreover, a project made by O. Briant and J. Guepet (2017)[6], which focuses on the integration of aircraft ground movements and taxiway operations. The Taxiway Sequencing Problem consists in ordering the sequence of takes-offs and landings on taxiways. There is a study of integration of these two problems with the aim of simultaneously increasing taxiway efficiency and reducing taxi times. Furthermore, a project performed by Y. Song and Y. Hui (2012)[7]. This paper investigates the effect induced by an aircraft during maneuvering for air-to-ground communication. Another project carried out by B. Mukherjee and M. Sinha (2017)[8], which studies the extreme aircraft maneuver under sudden lateral CG movement. Further, the effects of asymmetric center-of-gravity on some complex slip angle-of-attack maneuvers when turning. What is more, useful works made by M. Schmidt (2017) that study turn operations and simulations on aircrafts. An efficient aircraft turn is an essential component of airline success, especially for regional and short-haul operations. It is imperative that advancements in ground operations, specifically process reliability and passenger comfort. Furthermore, a similar project about maneuvers performed by G. Li and H. Zhang (2015)[9]. This project studies the maneuver characteristics and is analyzed from the perspectives of maneuver modes and maneuverability. Longitudinal skip maneuver mode, equilibrium glide mode,

lateral weaving maneuver mode and lateral turning maneuver mode are adopted to describe the maneuver process. Another project carried out by W. Zhao and S. Alam (2013)[10]. The focus of this paper is the terminal maneuvering area system which integrates arrival and departure operations. It also combines air and ground side resources to model and understand system-level vulnerabilities. Moreover, a project performed by C. Roos (2010)[11]. In this project, a non-standard strategy is developed in this paper in order to improve the ground control maneuvers of a civilian aircraft. In addition, a project made by S. Hamzah (2015)[12]. The purpose in this study is to analyze the optimization of aircraft parking and ground maneuvers stands, and proposed model for apron development in near future at Sultan Hasanuddin International Airport to achieve safety on airport operation activities. Furthermore, a paper performed by D. Lemay (2011)[13] In the following paper, a gain scheduled yaw controller is proposed to control low speed rolling and maneuvering of an aircraft on ground. This method is based on local linearization of a nonlinear model and the synthesis of a family of local controllers.

3. Modelling

In this chapter there is a fully study of the mathematical model to get the main equations of the aircrafts and then combine those equations with some centripetal physic equations in order to get the maximum velocity. More details are given in the following sections.

3.1. Mathematical model

In this section, details of the derivation and implementation of a fully parameterized mathematical model that describes an aircraft moving on the ground are given. Those model parameters could easily be adapted to represent almost any passenger aircraft.

The mathematical model has been derived via force and moment equations, coupled to relevant subsystem descriptions.

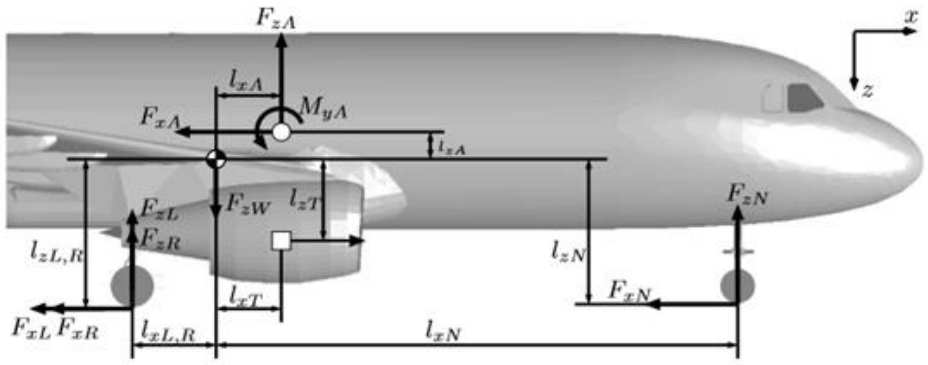

Figure 3-a Aircraft's body coordinate system (x, z)[14]

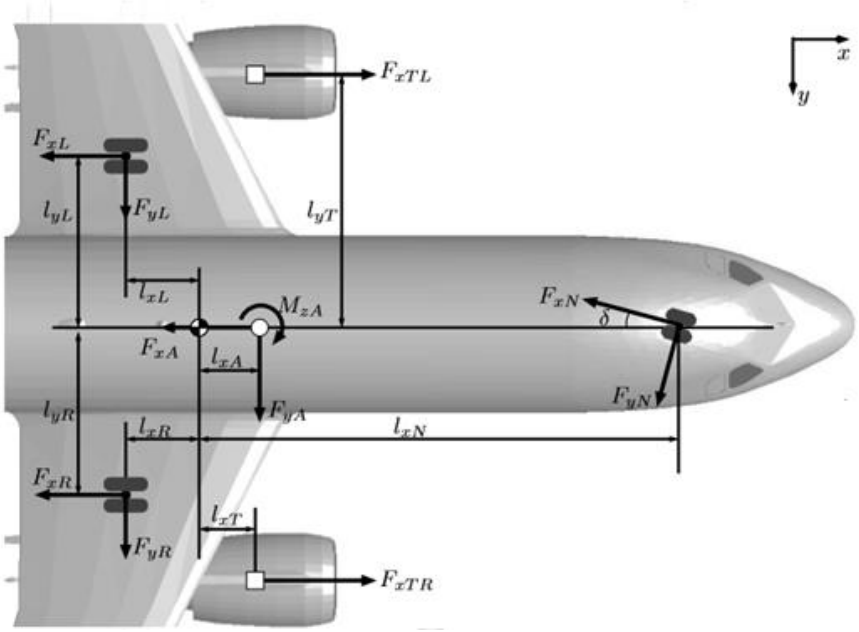

Figure 3-b Aircraft's body coordinate system (x, y)[14]

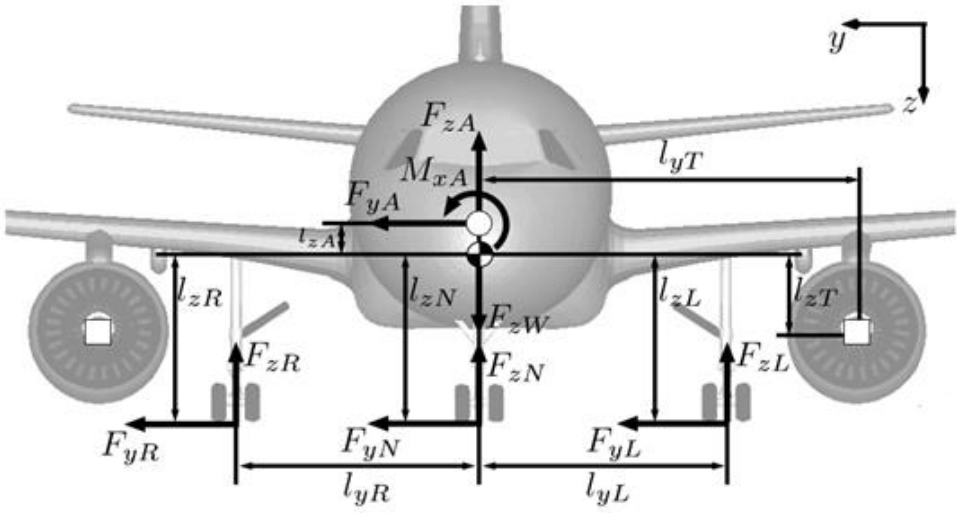

Figure 3-c Aircraft's body coordinate system (y, z)[14]

The aircraft has a tricycle configuration in which the nose gear is used for steering. On the aircraft there are two tires per gear. Due to the small separation distance they can be assumed to act in unison and, hence, are described as a single tire in the model. Throughout this study a conventional accepted coordinate systems for aircraft is used. Specifically, the positive x-axis points along the center-line of the fuselage toward the nose of the aircraft, the z-axis is toward the ground and the y-axis completes the right-handed body-fixed coordinate system. This body coordinate system is assumed to

coincide with the aircraft's principal axes of inertia, a reasonable assumption due to symmetries of the airframe. The equations of motion were derived from Newton's Second Law by balancing either the forces or moments.[5]

The equations of motion for the velocities in the body coordinate system of the aircraft are given as six ordinary differential equations:

$$m(a_x + V_zW_y - V_yW_z) = F_{xTL} + F_{xTR} - F_{xR} - F_{xL} - F_{xN}\cos(\delta) - F_{yN}\sin(\delta) - F_{xA} + F_zW\sin(\theta) \quad (3.1)$$

$$m(a_y + V_xW_z - V_zW_x) = F_{yR} + F_{yL} + F_{yN}\cos(\delta) - F_{xN}\sin(\delta) + F_{yA} + F_zW\sin(\phi)$$

$$m(a_z + V_yW_x - V_xW_y) = F_zW\cos(\theta)\cos(\phi) - F_{zR} - F_{zL} - F_{zN} - F_{zA}$$

$$I_{xx}W'_x - (I_{yy} - I_{zz})W_yW_z = I_{yL}F_{zL} - Iy_RF_{zR} - I_{zL}F_{yL} - I_{zR}F_{yR} - I_{zN}F_{yN}\cos(\delta) + I_{zN}F_{xN}\sin(\delta) + I_{zA}F_{yA} + M_{xA}$$

$$I_{yy}W'_y - (I_{zz} - I_{xx})W_xW_z = I_{xN}F_{zN} - I_{zN}F_{xN}\cos(\delta) - I_{zN}F_{yN}\sin(\delta) - I_{xR}F_{zR} - I_{zR}F_{xR} - I_{xL}F_{zL} - I_{zL}F_{x\,L} + I_{zT}F_{xTL} + I_{zT}F_{xTR} + I_{za}F_{xA} + I_{xA}F_{zA} + M_{yA}$$

$$I_{zz}W'_z - (I_{xx} - I_{yy})W_xW_y = I_{yR}F_{xR} - I_{yL}F_{xL} - I_{xR}F_{yR} - I_{xL}F_{yL} + I_{xN}F_{yN}\cos(\delta) - I_{xN}F_{xN}\sin(\delta) + I_{xA}F_{yA} + I_{yT}F_{xTL} - I_{yT}F_{xTR} + M_{zA}$$

Defining the velocities in the world axis as V_{xW}, V_{yW} and V_{zW}, the velocity transformation equations are given by:

$$\begin{pmatrix} V_{xW} \\ V_{yW} \\ V_{zW} \end{pmatrix} = \begin{bmatrix} C_\theta C_\psi & S_\phi S_\theta C_\psi - C_\phi S_\psi & C_\phi S_\theta C_\psi + S_\phi S_\psi \\ C_\theta S_\psi & S_\phi S_\theta S_\psi + C_\phi C_\psi & C_\phi S_\theta S_\psi - S_\phi C_\psi \\ -S_\theta & S_\phi C_\theta & C_\phi C_\theta \end{bmatrix} \begin{pmatrix} V_X \\ V_Y \\ V_Z \end{pmatrix} \quad (3.2)$$

Defining the angular velocities in the world axis as W_{xW}, W_{yW} and W_{zW}, the angular velocity transformation equations are given by:

$$\begin{pmatrix} W_{XW} \\ W_{YW} \\ W_{ZW} \end{pmatrix} = \begin{bmatrix} 1 & S_\theta S_\phi / C_\phi & C_\phi S_\theta / C_\theta \\ 0 & C_\phi & -S_\phi \\ 0 & S_\phi / C_\theta & C_\phi / C_\theta \end{bmatrix} = \begin{pmatrix} W_X \\ W_Y \\ W_Z \end{pmatrix} \quad (3.3)$$

3.2. Tire modelling

In order to calculate tire forces for the mathematical model it is necessary to calculate the local displacements and velocities of the tires. The model used here assumes that the roll axis of the tire is always parallel to the ground because the pitch and roll angles of the aircraft remain relatively small. It is therefore appropriate to use the velocities of the aircraft in the body coordinate system and Euler angles to calculate local displacements and velocities of the tires. This section focuses on these calculations that are used in obtaining the tire forces. [5]

Parameter	Description	Units	Nose	Main
m_t	mass of tyre	kg	21	75.5
k_z	stiffness coeff.	kN/m	1190	2777
ζ	damping ratio		0.1	0.1
c_z	damping coeff.	Ns/m	1000	2886

Table 3-a Parameters values used to calculate the vertical tire force[5]

In the model there are two tires per gear, although due to the small separation distance they can be assumed to act in unison, hence, they are described as a single tire in the rest of the paper. At lower velocities the forces generated by the tires have a dominant effect over aerodynamic forces on the motion of the aircraft. The vertical force component on the tire can be approximated by a linear spring and damper system.[5]

The total force is:

$$F_Z = -K_Z\delta_Z - c_Z V_Z = K_Z\delta_Z - 2\zeta\sqrt{m_t K_Z} \times V_Z \quad (3.4)$$

Where V_{zN} is the vertical velocity of the nose gear tyre, and δ_{zN} is the nose gear tire deflection representing the change in tire diameter between the loaded and unloaded condition. The stiffness coefficients k_z and damping coefficient c_z are specified in tables. Differences in the vertical velocity and deflection of each tire give the asymmetric load distribution between the gears.[15]

Also, notice that the operating pressure of the aircraft tire is almost 6 times that of the passenger tire; and that the aircraft tire is operating at a deflection of 32%, as compared to 11% for the passenger tire.

The vertical velocity of each tire can be calculated in terms of the velocities in the body coordinate system as:

$$V_{zN} = V_z - l_{xN}W_y \quad (3.5)$$

$$V_{zR} = V_z + l_{yR}W_x + l_{xR}W_y$$

$$V_{zL} = V_z - l_{yL}W_x + l_{xL}W_y$$

Where V_z is the local vertical velocity of the respective tyre.

The deflection of each tire is given in terms of the aircraft's position states in the world coordinate system as:

$$\delta_{zN} = -l_{zN} - Z + l_{xN}\theta \quad (3.6)$$

$$\delta_{zR} = -l_{zR} - Z - l_{xR}\theta - l_{yR}\phi$$

$$\delta_{zL} = -l_{zL} - Z - l_{xL}\theta + l_{yL}\phi$$

The longitudinal and lateral forces at the tire-ground interface depend on the vertical load acting on the tire and on its slip angle. The slip angle of a tire is the angle the tire

makes with its direction of motion. For each respective tire, the slip angle α is defined in terms of its local longitudinal velocity V_x and its local lateral velocity V_y as:[5]

$$\alpha = arctan(\frac{Vy}{Vx}) \quad (3.7)$$

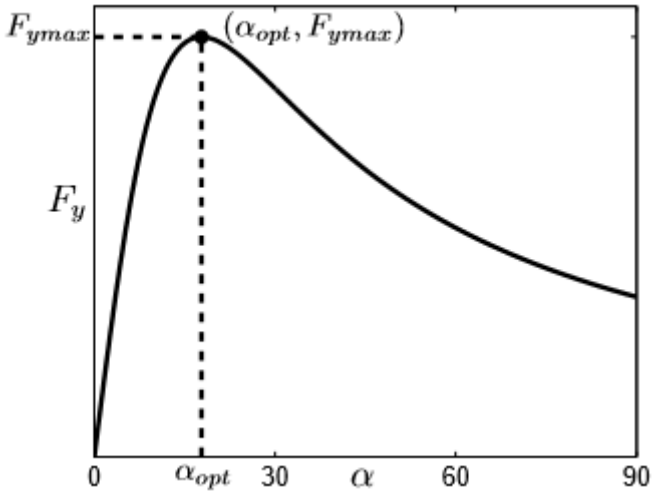

Figure 3-d Lateral force against slip angle[5]

Therefore, to find the slip angle it is necessary to find the longitudinal and lateral velocity of each tyre. These velocities are calculated in terms of the aircraft's velocities in the body coordinate system and the steering angle applied to the nose gear δ as:

$V_{xN} = V_x \cos(\delta)+(V_y + l_{xN}W_z)\sin(\delta)$ (3.8)

$V_{yN} = (V_y + l_{xN}W_z)\cos(\delta)-V_x \sin(\delta)$

$V_{xR} = V_x - l_{yR}W_z$

$V_{yR} = V_y - l_{xR}W_z$

$V_{xL} = V_x + l_{yL}W_z$

$V_{yL} = V_y - l_{xL}W_z$

Rolling resistance on hard surfaces is caused by hysteresis in the rubber of the tyre. The pressure in the leading half of the contact patch is higher than in the trailing half, and consequently the resultant vertical force does not act through the middle of the wheel. A horizontal force in the opposite direction of the wheel movement is needed to maintain equilibrium. This horizontal force is known as the rolling resistance. The ratio of the rolling resistance F_x, to vertical load F_z, on the tyre is known as the coefficient of rolling resistance μ_R, where a value of 0.02 is typically used for aircraft tyres. An adapted Coulomb friction model is used:[15]

$$F_X = -\mu_R F_Z \cos(\alpha) \qquad (3.9)$$

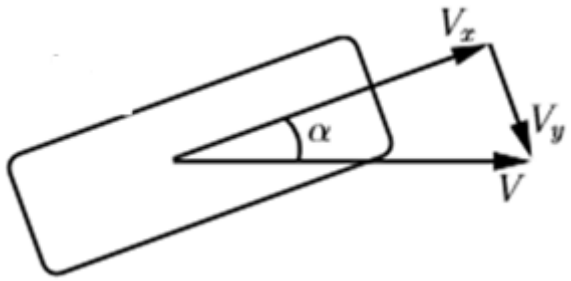

Figure 3-e Slip angle[5]

When no lateral force is applied to a tire, the wheel moves in the same direction as the wheel plane. When a side force is applied to the wheel it makes an angle with its direction of motion. This angle is known as the slip angle α, as depicted in Figure 3-5.

The lateral force on the respective tire Fy is a function of α and can be represented as:[5]

$$F_y(\alpha) = 2\frac{F_{ymax}\alpha_{opt}\alpha}{\alpha_{opt}^2 + \alpha^2} \qquad (3.10)$$

Where F_{ymax} is the maximum force that the tyre can generate and α_{opt} is the optimal slip angle at which this occurs. The parameters F_{ymax} and α_{opt} depend quadratically on the vertical force on the tyre F_z and, hence, change dynamically in the model. The

values for nose gear tyres F_{ymaxN} and α_{optN}, and main gear tyres $F_{ymaxR,L}$ and $\alpha_{optR,L}$ are obtained from the equations:

$$F_{ymaxN} = -3.53\times10-6F^2_{zN} + 8.83\times10-1F_{zN} \quad (3.11)$$

$$\alpha_{optN} = 3.52\times10 - 9F^2_{zN} + 2.80\times10-5F_{zN} + 13.8$$

$$F_{ymaxR,L} = -7.39\times10-7F^2_{zR,L} + 5.11\times10-1F_{zR,L}$$

$$\alpha_{optR,L} = 1.34\times10 - 10F^2_{zR,L} + 1.06\times10-5F_{zR,L} + 6.72$$

3.3. Equilibrium equations

A body is truly in equilibrium when it has no tendency to turn or move. This means no translation and no rotation.[16]

When a body is in equilibrium:

- The sum of the anticlockwise moments of any point is equal and opposite to the sum of the clockwise moments about that point.
- The resultant force in any direction is zero

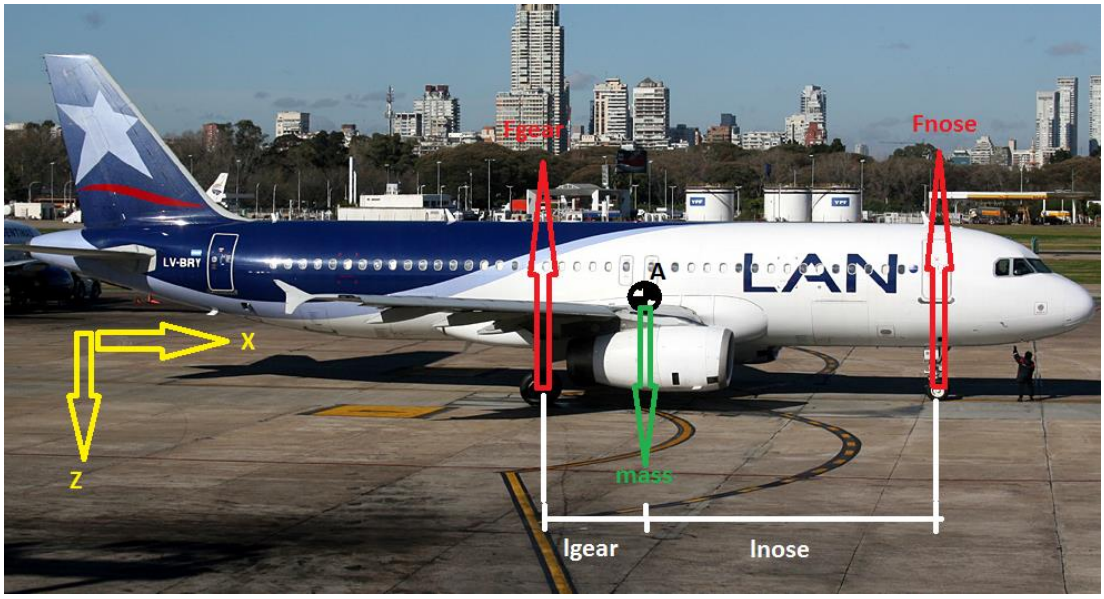

Table 3-b Aircraft Free Body Diagram

Using the principle of moments and taking moments about the point A (center of mass):

$$Clockwise\ moments = Anticlockwise\ moments$$

$$Fgear \times lgear = Fnose \times lnose \quad (3.12)$$

Balancing the vertical forces, the sum of vertical forces is zero

$$mass - Fgear - Fnose = 0 \quad (3.13)$$

3.4. Centripetal and Newton's equation

According to Isaac Newton's Second Law:

$$F = m \times a \qquad (3.14)$$

Where force is measured in Newtons, mass is measured in kilograms, and acceleration is measured in meters per second squared.[17]

The centripetal acceleration is the motion inwards towards the center of a circle. The acceleration is equal to the square of the velocity, divided by the radius of the circular path.[18]

$$a_c = \frac{v^2}{r} \qquad (3.15)$$

a_c = acceleration, centripetal, m/s^2

v = velocity, m/s

r = radius, m

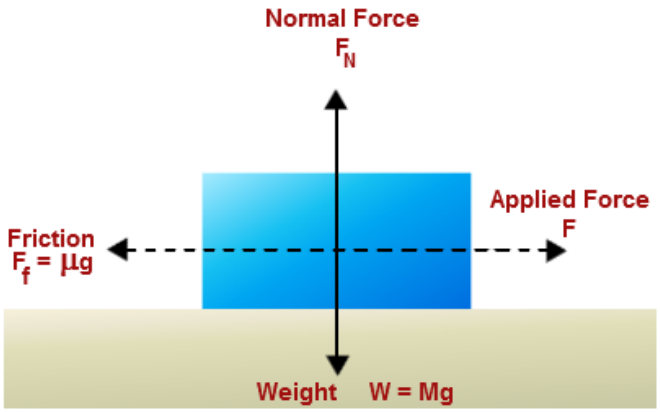

Figure 3-f Free Body DiagramFriction[22]

Friction is the retarding force coming into play when two bodies are in contact with each other, in our case, the tires of the aircraft with the ground. When turning, an aircraft should reduce its speed by 1/3 on wet roads.[19]

$$F_f = \mu_g \times N = \mu_g \times m \times g \quad (3.16)$$

$$F_f = m \times a.centripetal = m\frac{v^2}{r} \quad (3.17)$$

From the equation above, isolating the velocity:

$$v = \sqrt{\frac{r \times F_f}{m}} \quad (3.18)$$

Those maximum velocity calculations are done for the three types of aircrafts and each aircraft has a different mass and maximum friction force that the tire can resist.

In order to calculate the minimum radius that the taxiway should have with a fixed velocity, it is calculated isolating the radius with the same equation above.

$$r = \frac{v^2 \times m}{F_f} \quad (3.19)$$

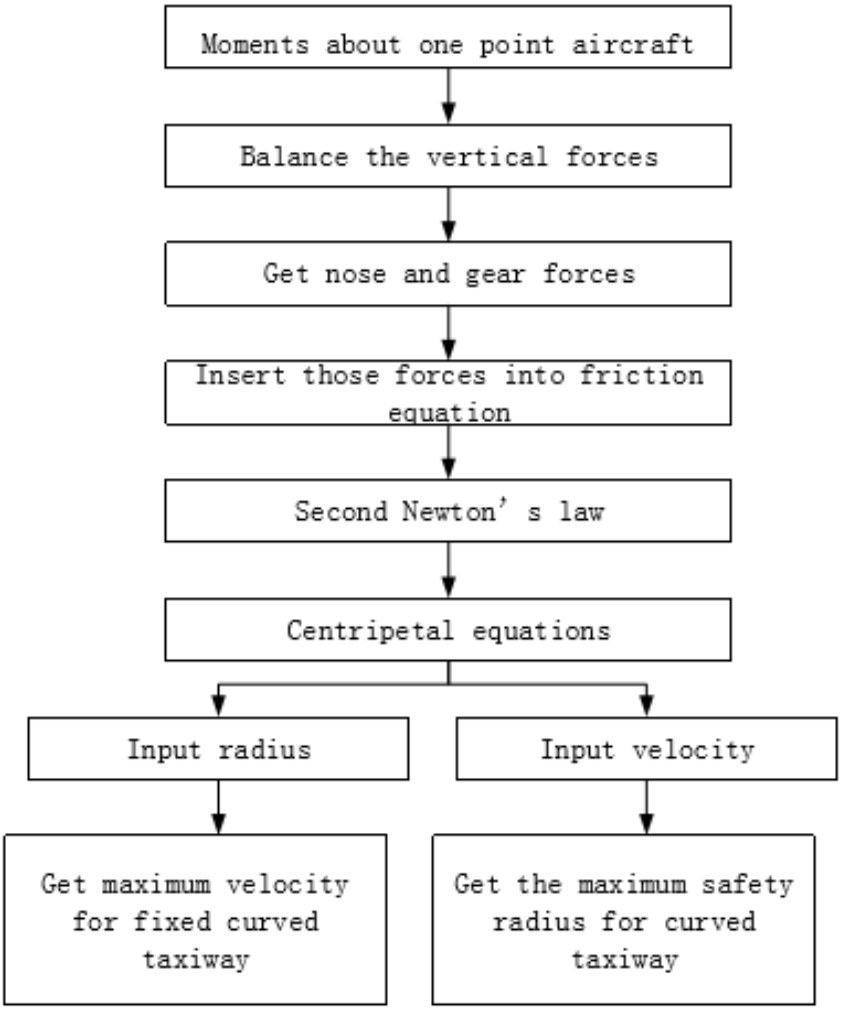
Moments about one point aircraft
Balance the vertical forces
Get nose and gear forces
Insert those forces into friction equation
Second Newton' s law
Centripetal equations
Input radius
Input velocity
Get maximum velocity for fixed curved taxiway
Get the maximum safety radius for curved taxiway

4. Data

In this chapter there is a fully explanation of the experimental design in order to understand how to get the results.

First of all, in the section 6.1 there is a complete explanation of the mathematical model, which some equations will be later used in the following section 6.2. At the end of the modelling part (6.2), an essential equation is found and will be used for the three types of aircraft. For all the calculations, all the parameters are given in tables and there is a list in chapter 3 with all the nomenclatures. Those parameters, which have been referenced, were found in books and other papers. The distances and maximum masses of the aircrafts were found in Airbus and Boeing web sites and are needed to make other calculations in section 6.3. Afterwards, the gear and nose forces for each type of aircraft are calculated with the equations 6.12 and 6.13 and then, those forces previously calculated are inserted in equation 6.11 in order to get the maximum friction force that the nose and gear can resist. Those maximum friction forces are not the same for each type of aircraft due the fact that the masses and thickness of the tires are different. Then, combining Second Newton's equation (6.14) and physics centripetal equations (6.17) two important equations are got in order to calculate the maximum speed (equation 6.18) and the minimum radius of the taxiway curvature (6.19). So as to make all the calculations the software Matlab is used in all the cases to insert all the parameters into the corresponding equations. The main Matlab code is given in chapter 11. In this code, all the parameters are introduced and inserted in the main equations. Some graphics are represented through Microsoft Excel in order to better understand the results calculated in Matlab.

5. Results

This is to understand better which parameters were used to calculate the gear and nose forces using the equations 6.12 and 6.13 because it is tricky to comprehend the Matlab code.

Where the maximum mass of the three planes are:[20]

m_{320}=75900kg; m_{380}=540000kg; m_{737}=70530kg.

Then, it is necessary to multiply those masses for the gravity in order to get the Weight

Where the gear and nose distances are:[21]

$lgear_{320}$=1.91; $lgear_{737}$=1.8145; $lgear_{380}$=7.608;

$lnose_{320}$=10.77; $lnose_{737}$=10.23; $lnose_{380}$=17.752;

Solving the equations with Matlab software the following gear and nose forces are got:

$Fgear_{320}$=6.3242e+05N; $Fgear_{380}$=3.1044e+06N; $Fgear_{737}$=5.8766e+05N

$Fnose_{320}$=1.1215e+05N; $Fnose_{380}$=2.1929e+06N; $Fnose_{737}$= 1.0423e+05N

In ZGHA airport there are two turns of 90 degrees each one on the taxiway. The first turn has a radius of 40 meters and the second turn of 60 meters. Below, there are the maximum velocities for dry and wet pavement.

Radius(m)	Velocity A320	Velocity A380	Velocity B737
40	23,69695044	20,3553169	26,91257716
60	29,02271852	24,93006998	32,96104086

Table 5-a Maximum velocities for dry curved taxiway

Radius(m)	Velocity A320	Velocity A380	Velocity B737
40	15,63998729	13,43450915	17,76230093
60	19,15499422	16,45384619	21,75428696

Table 5-b Maximum velocities for wet curved taxiway

5.1. Sensitivity Analysis

5.1.1. Dry Sensitivity Analysis

Radius (m)	Velocity A320 (km/h)	Velocity A380 (km/h)	Velocity B737 (km/h)
20	16,75627435	14,39338261	19,03006581
40	23,69695044	20,3553169	26,91257716
60	29,02271852	24,93006998	32,96104086
80	33,5125487	28,78676523	38,06013162
100	37,46816849	32,18458195	42,55252077
120	41,04432214	35,25644308	46,61395101
140	44,33293483	38,08131092	50,34882157
160	47,39390088	40,7106338	53,82515433
180	50,26882305	43,18014784	57,09019743
200	52,98799204	45,5158723	60,17835199
220	55,5742749	47,7374496	63,11558803

Table 5-c Maximum velocity for dry fixed curved taxiway

According to the results, the velocity tends to increase when the radius of the curvature is larger. Moreover, the results also show that the smallest and lighter aircraft (B737) can achieve a higher speed when turning at the same radius than the others. Alternatively, the biggest and heavier aircraft (A380) must increase the velocity to do the same turn. Therefore, with a fixed radius curvature, there is a relation which lighter aircrafts can achieve higher velocities than heavier aircrafts when turning.

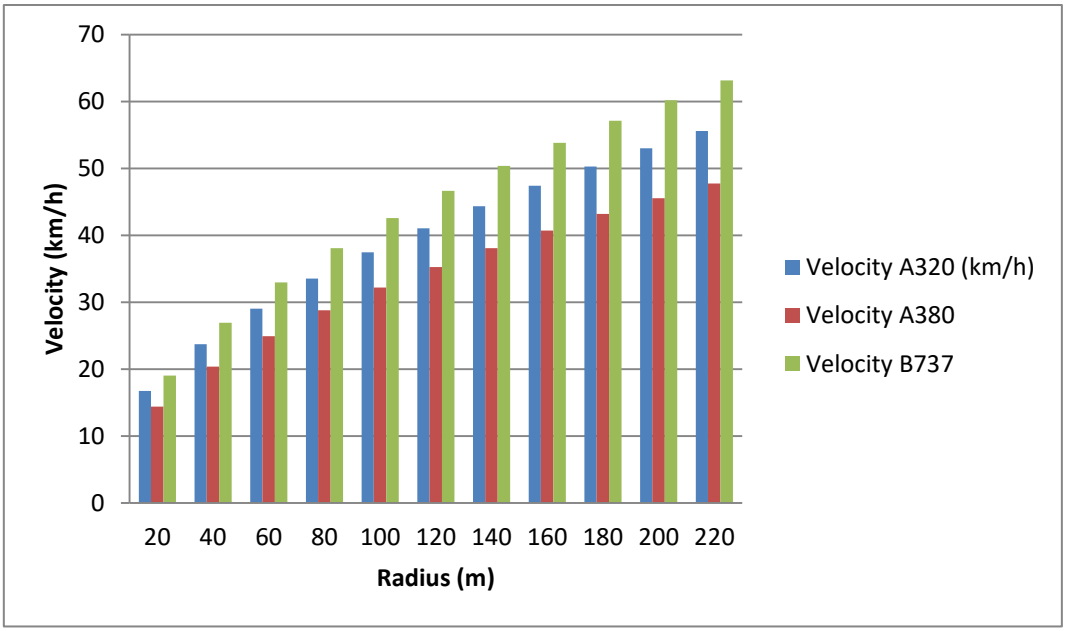

Figure 5-a Aircraft maximum dry velocities with a fixed radius

This graphic is made from the table above in order to facilitate the comparison and make it easier to understand. In the vertical axis is shown the velocity of the aircraft in km/h and in the horizontal axis the radius in meters.

For new airports that would like to save time when operating with fixed velocity, some new turning calculations are given. Basically, those calculations show the minimum radius that the taxiway curvature should have for a fixed velocity. If the radius is smaller than the results shown, the friction force that can resist the tires will not be enough, and the aircraft may lose control.

Velocity (km/h)	Radius A320 (m)	Radius A380 (m)	Radius B737 (m)
5	1,780799723	2,41348311	1,380668524
10	7,123198894	9,653932439	5,522674095
15	16,02719751	21,72134799	12,42601671
20	28,49279557	38,61572976	22,09069638
25	44,51999309	60,33707774	34,51671309
30	64,10879004	86,88539195	49,70406685
35	87,25918645	118,2606724	67,65275766
40	113,9711823	154,462919	88,36278551
45	144,2447776	195,4921319	111,8341504
50	178,0799723	241,348311	138,0668524
55	215,4767665	292,0314563	167,0608914
60	256,4351602	347,5415678	198,8162674
65	300,9551533	407,8786455	233,3329805

Table 5-d Minimum safety radius for dry curved taxiway

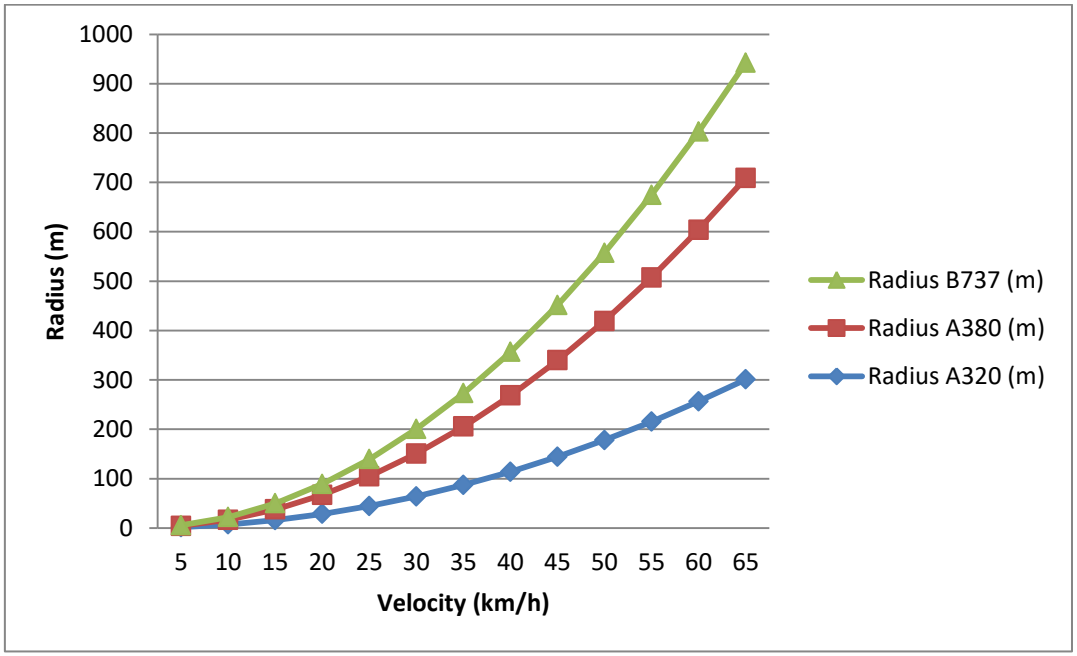

Figure 5-b Minimum dry safety radius with a fixed velocity

This line graphic is made from the table above in order to facilitate the comparison. In the vertical axis there is radius of the aircraft in meters and in the horizontal axis the fixed velocity in km/h.

5.1.2.Wet Sensitivity Analysis

In this section there are the same calculations and table's format than in the section above, but changing the friction parameter and considering that the aircraft is turning on a wet taxiway.

Radius (m)	Velocity A320 (km/h)	Velocity A380 (km/h)	Velocity B737 (km/h)
20	11,05914107	9,499632525	12,55984344
40	15,63998729	13,43450915	17,76230093
60	19,15499422	16,45384619	21,75428696
80	22,11828214	18,99926505	25,11968687
100	24,72899121	21,24182409	28,08466371
120	27,08925261	23,26925243	30,76520767
140	29,25973699	25,13366521	33,23022224
160	31,27997458	26,86901831	35,52460185
180	33,17742321	28,49889758	37,67953031
200	34,97207475	30,04047571	39,71771231
220	36,67902143	31,50671673	41,6562881

Table 5-e Aircraft maximum wet velocities with a fixed radius

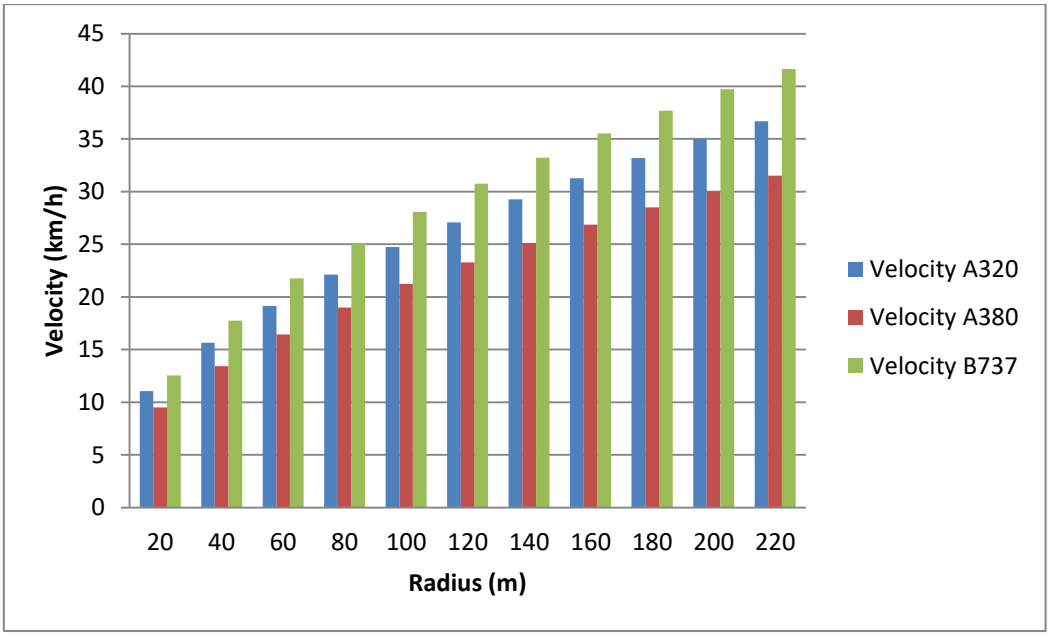

Figure 5-c Minimum wet taxiway curvature radius with a fixed velocity

Velocity (km/h)	Radius A320 (m)	Radius A380 (m)	Radius B737 (m)
5	4,088153635	5,540594834	3,169578796
10	16,35261454	22,16237934	12,67831518
15	36,79338272	49,86535351	28,52620917
20	65,41045816	88,64951735	50,71326074
25	102,2038409	138,5148709	79,23946991
30	147,1735309	199,461414	114,1048367
35	200,3195281	271,4891469	155,309361
40	261,6418326	354,5980694	202,853043
45	331,1404444	448,7881816	256,7358825
50	408,8153635	554,0594834	316,9578796
55	494,6665898	670,4119749	383,5190343
60	588,6941234	797,8456561	456,4193467
65	690,8979643	936,360527	535,6588166

Table 5-f Minimum safety radius for wet curved taxiway

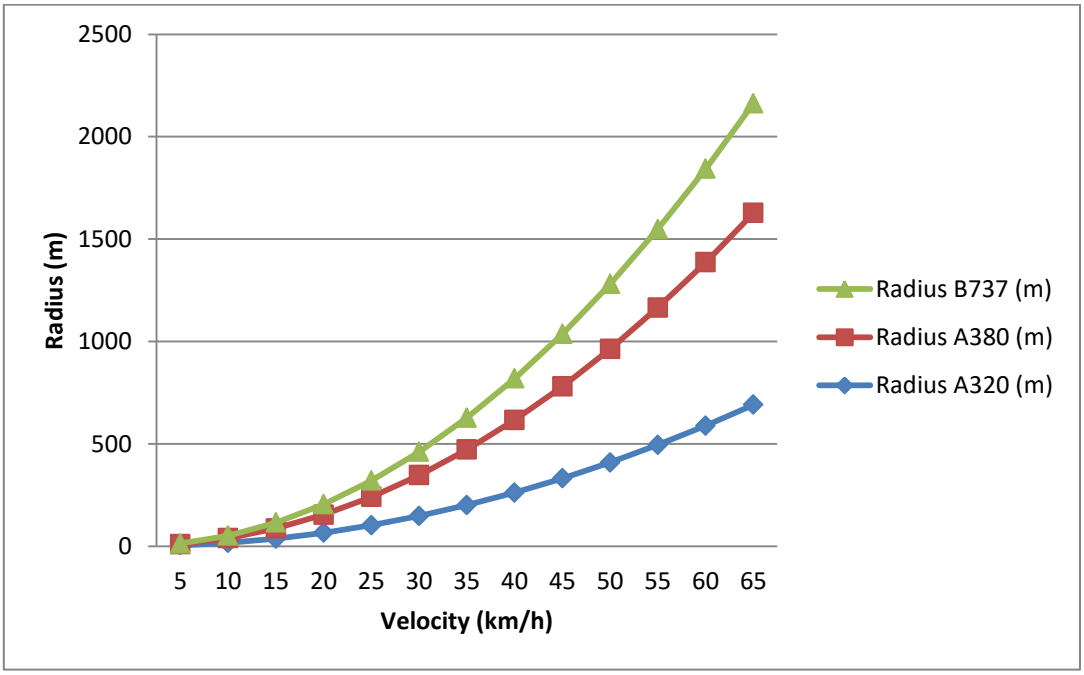

Figure 5-d Minimum wet safety radius with a fixed velocity

6. Conclusions

The realization of this project has conducted to several conclusions that will be explained in this chapter.

According to the results, the velocity tends to increase when the radius of the curvature is larger. Moreover, the results also show that the smallest and lighter aircraft (B737) can achieve a higher speed when turning. Alternatively, the biggest and heavier aircraft (A380) must decrease the velocity to do the same turn. Therefore, with a fixed radius curvature, there is a relation in which lighter aircrafts can achieve higher velocities than heavier aircrafts when turning.

The results also show that aircrafts must slow down 1/3 of theirs velocity while turning on wet taxiways. In addition, the results indicate that the nose gear supports about 15% of the total weight of the aircraft and hence, the main gears (right and left) resist the other 85% of the total mass.

In accordance with the minimum radius that a taxiway curvature must have with a fixed velocity, the minimum radius tends to increase when the velocity is higher. Moreover, the results also show that the smallest and lighter aircraft (B737) needs a smaller radius when turning at the same velocity than the other aircrafts. Alternatively, the biggest and heavier aircraft (A380) must provide a larger radius taxiway infrastructure so as to make the same turn. Thus, with a fixed velocity, results show a relationship in which lighter aircrafts require a smaller radius than heavier aircrafts when turning.

7. Bibliography

1. Corporation, S. Airport Operations. *Technology* **23,** 1–17 (2007).

2. Of, C. & Distance, M. L. Calculation of Minimum Line-Up Distance Correction. 1–5 (2012).

3. Aviation, I. C. ICAO Annex 14 Aerodromes. **1,** 1–39 (2004).

4. AACG. A380 infrastruture reqs. (2004).

5. Rankin, A., Krauskopf, B., Lowenberg, M. & Coetzee, E. Bifurcation and stability analysis of aircraft turning manoeuvres. *J. Guid. Control Dyn.* **32,** 1–24 (2008).

6. Guépet, J., Briant, O., Gayon, J.-P. & Acuna-Agost, R. Integration of aircraft ground movements and runway operations. *Transp. Res. Part E Logist. Transp. Rev.* **104,** 131–149 (2017).

7. Meng, Y. S. & Lee, Y. H. Study of shadowing effect by aircraft maneuvering for air-to-ground communication. *AEU - Int. J. Electron. Commun.* **66,** 7–11 (2012).

8. Mukherjee, B. K. & Sinha, M. Extreme aircraft maneuver under sudden lateral CG movement: Modeling and control. *Aerosp. Sci. Technol.* **68,** 11–25 (2017).

9. Li, G., Zhang, H. & Tang, G. Maneuver characteristics analysis. *Aerosp. Sci. Technol.* **43,** 321–328 (2015).

10. Zhao, W., Alam, S. & Abbass, H. A. Evaluating ground vulnerabilities in an integrated terminal maneuvering area using co-evolutionary computational red teaming. *Transp. Res. Part C Emerg. Technol.* **29,** 32–54 (2013).

11. Roos, C., Biannic, J.-M., Tarbouriech, S., Prieur, C. & Jeanneau, M. On-ground aircraft control design using a parameter-varying anti-windup approach. *Aerosp. Sci. Technol.* **14,** 459–471 (2010).

12. Hamzah, S. & Adisasmita, S. A. Aircraft taxiway Stands: Proposed Model for Indonesian Airports. *Procedia Environ. Sci.* **28,** 324–329 (2015).

13. Lemay, D., Chamaillard, Y., Basset, M. & Garcia, J. P. Gain-Scheduled Yaw Control for Aircraft Ground Taxiing. *IFAC Proc. Vol.* **44,** 12970–12975 (2011).

14. Rankin, J. Bifurcation Analysis of Nonlinear Ground Handling of Aircraft. (2010).

15. Coetzee, E. Modelling and Nonlinear Analysis of Aircraft Ground Manoeuvres. 1–123 (2011).

16. Equilibrium. Available at: http://www.schoolphysics.co.uk/age16-19/Mechanics/Statics/text/Equilibrium_/index.html. (Accessed: 9th June 2017)

17. Force, Mass, Acceleration | Zona Land Education. Available at: http://zonalandeducation.com/mstm/physics/mechanics/forces/newton/mightyFEqMA/mightyFEqMA.html. (Accessed: 8th June 2017)

18. Centripetal Acceleration Formula. Available at: http://www.softschools.com/formulas/physics/centripetal_acceleration_formula/71/. (Accessed: 8th June 2017)

19. Aircraft Manoeuvres wet safety Administration. Available at: https://cms.fmcsa.dot.gov/safety/driver-safety/cmv-driving-tips-too-fast-conditions.

20. Airbus.com | Airbus, Commercial Aircraft. Available at: http://www.airbus.com/es/. (Accessed: 13th June 2017)

21. Boeing: The Boeing Company. Available at: http://www.boeing.com/. (Accessed: 13th June 2017)

22. Free Body Diagrams | Friction | Force. Available at: https://es.scribd.com/document/95647917/Free-Body-Diagrams. (Accessed: 16th June 2017)

8. Matlab code

```
lmac=4.194;

lxn=10.186+0.3*lmac;

lzn=2.932;

lxr=2.498-0.3*lmac; lxl=2.498-0.3*lmac;

lyr=3.795; lyl=3.795;

lzr=2.932; lzl=2.932;

lxa=(0.25-0.3)*lmac;

lza=0.988;

lxt=(0.25-0.3)*lmac;

lytr=5.755; lytl=5.755;

lzt=1.229;

m=75900;

mtn=21; mtm=75.5;

kzn=1190000; kzm=2777000;

Cdamp=0.1;

czn=1000; czm=2886;

deltaz=0.055;

rollingcoef=0.02;

Sw=122.4;

airdensity=1.225;
```

```
E=0.01;

m320=75900;

m380=540000;

m737=70530;

g=9.81;

lgear320=1.91;

lgear737=1.8145;

lgear380=7.608;

lnose320=10.77;

lnose737=10.23;

lnose380=17.752;

Fz320=m320*g;

Fz380=m380*g;

Fz737=m737*g;

Fzn320=(Fz320*lgear320)/(lgear320+lnose320);

Fzn380=(Fz380*lgear380)/(lgear380+lnose320);

Fzn737=(Fz737*lgear737)/(lgear737+lnose737);

Fzg320=Fz320-Fzn320;

Fzg380=Fz380-Fzn380;

Fzg737=Fz737-Fzn737;

Ffn320=-0.00000353*(Fzn320^2)+0.883*Fzn320;

Ffn380=-0.00000353*(Fzn380^2)+5.6917*Fzn380;
```

```
Ffn737=-0.00000353*(Fzn737^2)+0.883*Fzn737;

Ffg320=-0.000000739*(Fzg320^2)+0.511*Fzg320;

Ffg380=-0.000000739*(Fzg380^2)+2.8217*Fzg380;

Ffg737=-0.000000739*(Fzg737^2)+0.511*Fzg737;

Fft320=Ffn320+Ffg320;

Fft380=Ffn380+Ffg380;

Fft737=Ffn737+Ffg737;

r=40;

Vdry320=sqrt((Fft320*r)/m320)*3.6;

Vdry380=sqrt((Fft380*r)/m380)*3.6;

Vdry737=sqrt((Fft737*r)/m737)*3.6;

Vwet320=sqrt((Fft320*r)/m320)*3.6*0.66;

Vwet380=sqrt((Fft380*r)/m380)*3.6*0.66;

Vwet737=sqrt((Fft737*r)/m737)*3.6*0.66;
```